



NONLINEAR QUASI-STATIC FINITE ELEMENT ANALYSIS OF FLAT PLATE USING DAMAGE PLASTICITY MODEL

S. M. M. Islam⁽¹⁾, I. Anam⁽²⁾, H. M. G. Samdani⁽³⁾, Y. Sanada⁽⁴⁾, S. Takahashi⁽⁵⁾

⁽¹⁾ Junior Research Consultant, SATREPS-TSUIB Project, HBRI, Bangladesh, sheikh.muhammadul@gmail.com

⁽²⁾ Professor, Department of Civil Engineering, University of Asia Pacific, iftekhkar@uap-bd.edu

⁽³⁾ Graduate Student, Graduate School of Engineering, Osaka University, golam_samdani@arch.eng.osaka-u.ac.jp

⁽⁴⁾ Professor, Graduate School of Engineering, Osaka University, sanada@arch.eng.osaka-u.ac.jp

⁽⁵⁾ Associate Professor, Faculty of Engineering, Daido University, susumu-t@daido-it.ac.jp

Abstract

Flat slabs have become very popular in Bangladesh mainly due to their aesthetic view and satisfactory behavior under vertical loading. But since they are quite vulnerable in earthquakes, repair and retrofit are the only options they have of withstanding the stresses due to major earthquakes. Nonlinear Quasi-Static Analysis of flat slabs is performed in this work to check the performance against punching, comparing numerical results with experimental observations from reversible load tests. Since punching shear is the most damaging of the possible seismic distresses, this study focuses on simulating punching shear failure due to earthquake. Numerical simulations are illustrated using computational modeling by the well-known software ABAQUS to obtain outputs for understanding seismic performance of flat plate structural system. Finite element method (FEM) incorporating Concrete Damage Plasticity (CDP) model accomplishes the numerical simulation. The CDP model is used to perform the iterations at nonlinear stages and visualize real-time crack pattern and failure type of structural system.

Evaluating models are simulated as Reinforced Concrete (RC) flat plate structure, comparing with flat plate strengthened by using Wing Walls. Three-dimensional quasi-static nonlinear finite element analysis exhibits numerical solutions that predict the experimental outputs with visualization of localized failure patterns as well. The results are promising and numerical simulations reasonably satisfy the experiments. Before retrofit, the maximum load from numerical simulation was 5.98 kN compared to experimental result of 6.08 kN. The corresponding values came out to be 15.93 kN and 16.60 kN respectively after strengthening. The adaptability of CDP model in nonlinear seismic evaluation by FEM can have broad acceptance since the procedure is able to bypass analytical complexity, assure accuracy of numerical simulation and visualize failure pattern, validating the performance of such sophisticated and complex physical systems.

Keywords: Quasi-Static; Seismic performance; Finite element method; CDP; Failure Pattern



1. Introduction

Distinct explanation of the concrete behavior has always been a challenging part in the numerical simulation of the reinforced concrete structures specially for flat plate structure due to its unbalanced stress transformations. Several concrete material models are developed by researchers to overcome this critical state targeting simulating the concrete behavior precisely as under various loading and structural conditions. Concrete Damaged Plasticity (CDP) model of the ABAQUS standard software [1] is one of those concrete material models which has been developed based on works conducted by Lubliner *et al.* (1989) [4]. This model has a unique feature that characterizes its functionality from the other existing concrete models; the CDP model is formulated within a multi-purpose finite element FEM analysis software (ABAQUS).

The identification of input constitutive parameters which describes the material properties is basic idea. A numerical strategy for solving any boundary value problem (BVP) with location of crack, should consider a complex constitutive structural modelling. If structural material such as concrete is taken for research purpose, it is necessary to identify a large number of parameters. The notion of concrete constitutes a wide range of materials, whose properties are quantitatively and qualitatively different for typical tests (compression, tension and damage parameters). Recently, modelling of failure and crack has become one of the fundamental issues in structural analysis particularly in concrete structures. In this paper, a scalar variable is used to model the failure (in both compression and tension). The main task in simulation of experimental load and deformation capacity and failure description are the recognition of accuracy of values and crack patterns.

Development by [1,3,5], the constitutive equation in Eq. (1), (2) and (3) of material with scalar isotropic damage takes the following form:

$$\sigma = (1 - d)D_0^{el} : (\varepsilon - \varepsilon^{pl}) = D^{el} : (\varepsilon - \varepsilon^{pl}), \quad (1)$$

where σ is Cauchy stress tensor, by d is the scalar stiffness degradation variable, respectively, ε is the strain tensor, D_0^{el} the initial (undamaged) elastic stiffness of the material, while $D^{el} = (1-d)D_0^{el}$ is the degraded elastic stiffness tensor. The effective stress tensor is defined as:

$$\bar{\sigma} = D^{el} : (\varepsilon - \varepsilon^{pl}), \quad (2)$$

where ε^{pl} is the plastic strain. In the formulation, it is necessary to propose the evolution of the scalar degradation variable:

$$d = d(\bar{\sigma}, \tilde{\varepsilon}^{pl}) \quad (3)$$

governed by a set of effective stress tensor $\bar{\sigma}$ and hardening (softening) variables $\tilde{\varepsilon}^{pl}$. In CDP model, the stiffness degradation is initially isotropic and defined by degradation variable d_c in a compression zone and variable d_t in a tension zone in Eq. (4). When the structure is unloaded from anypoint on the strain softening branch of the stress-strain curves, the unloading response is observed to be weakened, the elastic stiffness of the material appears to be damaged (or degraded). The degradation of the elastic stiffness is significantly different between tension and compression tests. In either case, the effect is more pronounced as the plastic strain increases. The degraded response of concrete is characterized by two independent uniaxial damage variables, and which are assumed to be functions of the plastic strains, temperatura (θ), and field (f_i) variables:

$$d_t = d_t(\tilde{\varepsilon}_t^{pl}, \theta, f_i), (0 \leq d_t \leq 1); d_c = d_c(\tilde{\varepsilon}_c^{pl}, \theta, f_i), (0 \leq d_c \leq 1). \quad (4)$$

The uniaxial degradation variables are increasing functions of the equivalent plastic strains. They can take values ranging from zero, to one for the undamaged and fully damaged material respectively.

Thus, finally, the Cauchy stress tensor in Eq. (5) and (6) is related to the effective stress tensor $\bar{\sigma}$ through the scalar degradation parameter (1- d):

$$\sigma = (1 - d)\bar{\sigma} \quad (5)$$



Damage states in tension and compression are characterized independently by two hardening variables, $\tilde{\varepsilon}_t^{pl}$ and $\tilde{\varepsilon}_c^{pl}$, which are referred to equivalent plastic strains in tension and compression, respectively. The evolution of the hardening variables is given by the following expression:

$$\tilde{\varepsilon}^{pl} = \begin{bmatrix} \tilde{\varepsilon}_c^{pl} \\ \tilde{\varepsilon}_t^{pl} \end{bmatrix} \text{ and } \dot{\tilde{\varepsilon}}^{pl} = h(\bar{\sigma}, \tilde{\varepsilon}^{pl}) \cdot \dot{\varepsilon}^{pl} . \quad (6)$$

Cracking (tension) and crushing (compression) in concrete are represented by increasing values of the hardening (softening) variables. These variables control the evolution of the yield surface and the degradation of the elastic stiffness.

The yield function represents in Eq. (7), a surface in effective stress space which determines the states of failure or damage. For the inviscid plastic-damage model the yield function arrives at:

$$F(\bar{\sigma}, \tilde{\varepsilon}^{pl}) \leq 0. \quad (7)$$

Plastic flow is governed by a flow potential function $G(\bar{\sigma})$ according to non associative flow rule by Eq. (8):

$$\dot{\varepsilon}^{pl} = \dot{\lambda} \frac{\partial G(\bar{\sigma})}{\partial \bar{\sigma}} \quad (8)$$

The plastic potential function G is also defined in the effective stress space. $\dot{\lambda}$ is hardening parameter expresses the increment of plastic strain. For a full definition of CDP model in Abaqus the some obligatory parameters need to input described in the research work of Szczecina M. and Winnicki A. (2015) [8] as dilation angle ψ in the effective and deviator stress plane, flow potential eccentricity E , the ratio of biaxial compressive yield stress (f_{bo}) to uniaxial compressive yield stress (f_{co}) and the ratio of the second stress invariant (\bar{q}_{TM}) on the tensile meridian to that on the compressive meridian (\bar{q}_{CM}) for the yield function. There are also some optional parameters, namely, viscosity parameter, damage conditions for compression and tension, the viscosity parameter in tension test and dilation angle in compression test. Constitutive model of concrete (CDP) is one of the possible concepts. The behavior of concrete depends on material parameters and FEM adopting CDP can predict the experimental results in case of flat plate structure which are identified in the paper.

2. Numerical Computations and Comparison

In the computations of the standard applications, the finite element code, implemented in ABAQUS/Explicit is used. The models and the computations lead to the estimation of the propagation and the end stage of fracture in flat plate with retrofit option. The scalar damage variable in tension is used to compare crack patterns for the numerical and experimental models.

The following numerical investigation, which can verify the experiment of flat plate structure with simulations for the specimen, its geometry is as shown in Fig. 1. This analysis verifies the concrete CDP model for the case of dominant shearing for punching effect in the experiment. In the numerical simulation the clockwise and anti-clockwise quasi-static forces are applied by the rigid linear steel surface to the concrete specimen is shown in Fig. 2(c,d), thus, Fig. 2(e) demonstrates the pressure forces are distributed in a specific way as displacement controlled cyclic loading in FEM analysis. The reinforcements are in embedded constrained condition inside concrete parts. The constraint has a kinematic character and between the concrete specimen and the rigid surface, where the load is applied, contact conditions are perceived.

The computations were performed for the different mesh densities. After the mesh convergence check, the analysis with dominant eight-node three dimensional solid elements have been computed, the average mesh element size considered as 20mm x 20mm in all cases. In Fig. 2(a,b) the mesh with the dominant eight-node, plane stress elements is presented for both retrofitted and non-retrofitted conditions. An isotropic plastic model is considered for the reinforcements and the properties are shown in Table 4.

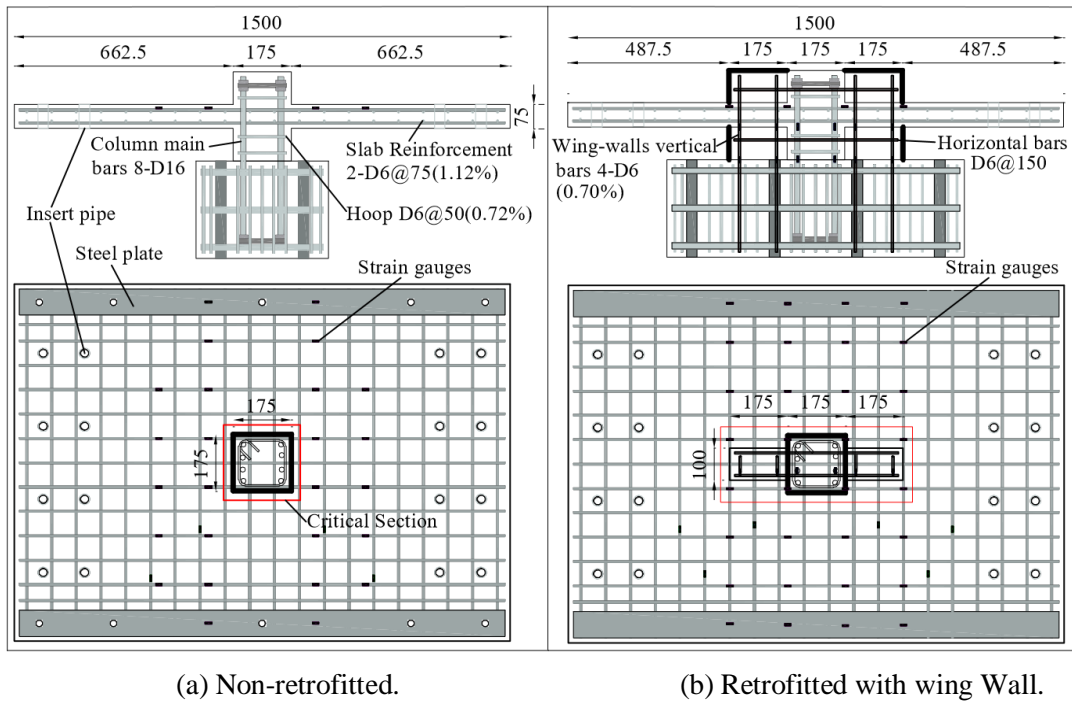
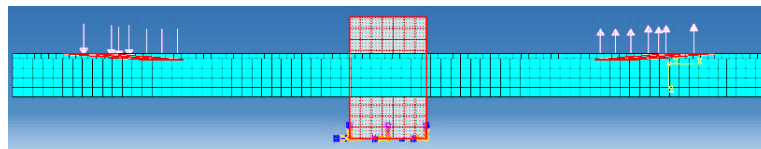
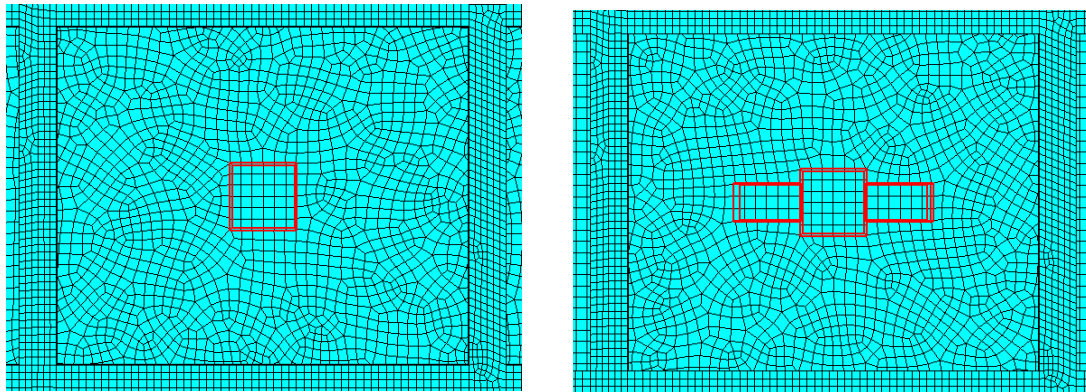
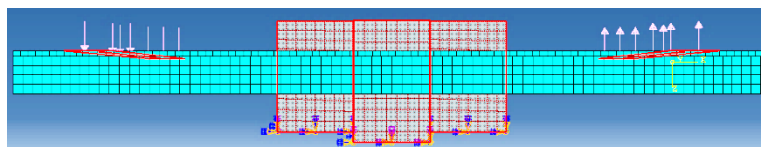


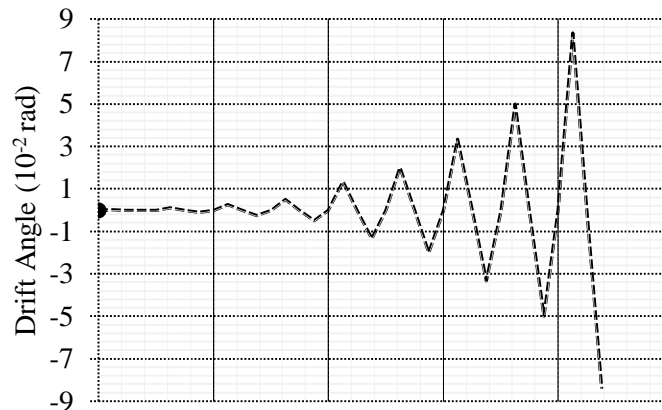
Fig. 1- The geometry of flat plate [7].



(c) Anti-clockwise loading and fixed support condition of non-retrofitted specimen.



(d) Anti-clockwise loading and fixed support condition of retrofitted specimen.



(e) Loading History [7].

Fig. 2- FEM model, Mesh Convergence and Loading State in ABAQUS.

The basic material properties including Abaqus inputs for steel model is shown in Table 1. The CDP parametric data is prepared through interpolations and shown in Table 2, 3 with following references. The Poisson's ratio of concrete for low strength is taken as 0.2 and for high strength 0.18. For Steel the Poisson's ratio is 0.3 for all cases. Table 1- Basic averaged material properties of concrete and steel [7].

Averaged Concrete Properties						
Type	Compressive strength (MPa)	Elastic modulus (GPa)	Crushing Strain %			
Non-retrofitted & Retrofitted	7.045	8.6	0.0017			
Wing Wall	37.04	30.93	0.0019			
Averaged Steel Properties						
Diameter (mm)	Yield stress (MPa)	Elastic modulus (GPa)	Tensile strength (MPa)			
6 & 16	375	183	520.5			
Abaqus Isometric Plastic Model input for steel						
Yield stress (MPa)	375	375	404	462	520	218
Plastic strain %	0	0.002	0.019	0.046	0.09	0.108

Table 2- The material parameters of CDP model for concrete $f'_c = 37.04 \text{ MPa}$ [2,6].

Material's parameters	$f'_c = 37.04 \text{ MPa}$	The parameters of CDP model	
		$\psi = \text{Dilatation Angle}$	35°
Concrete elasticity		$E = \text{Eccentricity}$	0.1
$E \text{ (GPa)}$	30.93	$F = f_{bo}/f_{co}$	1.12
Poisson's ratio	0.18	$K_c = \bar{q}_{TM}/\bar{q}_{CM}$	0.67
Concrete compression hardening		Concrete compression damage	



Stress [MPa]	Inelastic strain %	Damage Parameter (d_c)	Inelastic strain %
11.11	0	0	0
14.96	0.003	0.08	0.003
22.22	0.004	0.2	0.004
29.85	0.005	0.31	0.005
37.04	0.006	0.4	0.006
29.80	0.007	0.48	0.007
14.98	0.008	0.54	0.008
9.893	0.009	0.58	0.009
8.61	0.01	0.6	0.01
7.60	0.011	0.6	0.011
6.80	0.012	0.6	0.012
Concrete tension stiffening		Concrete tension damage	
Stress [MPa]	Inelastic strain %	Damage Parameter (d_t)	Inelastic strain %
3.5	0	0	0
3.15	0.0000224	0.1	0.0000224
2.45	0.000269	0.3	0.000269
1.75	0.000448	0.5	0.000448
1.05	0.000628	0.7	0.000628
0.35	0.000807	0.9	0.000807

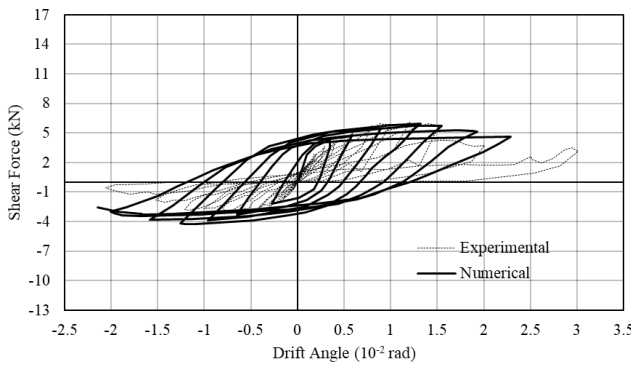
Table 2- The material parameters of CDP model for concrete $f'_c = 7.045 \text{ MPa}$ [2,6].

Material's parameters	$f'_c = 7.045 \text{ MPa}$	The parameters of CDP model	
		$\psi = \text{Dilatation Angle}$	35°
Concrete elasticity		$E = \text{Eccentricity}$	0.1
$E \text{ (GPa)}$	30.93	$F = f_{bo}/f_{co}$	1.12
Poisson's ratio	0.2	$K_c = \bar{q}_{TM}/\bar{q}_{CM}$	0.67
Concrete compression hardening		Concrete compression damage	
Stress [MPa]	Inelastic strain %	Damage Parameter (d_c)	Inelastic strain %
2.11	0	0	0
2.84	0.003	0.08	0.003
4.22	0.004	0.2	0.004
5.67	0.005	0.31	0.005
7.04	0.006	0.4	0.006
5.66	0.007	0.48	0.007
2.84	0.008	0.54	0.008
1.88	0.009	0.58	0.009
1.63	0.01	0.6	0.01

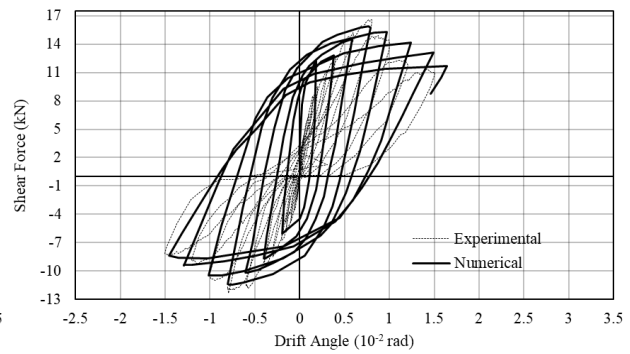


1.44	0.011	0.6	0.011
1.29	0.012	0.6	0.012
Concrete tension stiffening		Concrete tension damage	
Stress [MPa]	Inelastic strain %	Damage Parameter (d_t)	Inelastic strain %
0.66	0	0	0
0.59	0.000224	0.1	0.000224
0.46	0.000269	0.3	0.000269
0.33	0.000448	0.5	0.000448
0.19	0.000628	0.7	0.000628
0.066	0.000807	0.9	0.000807

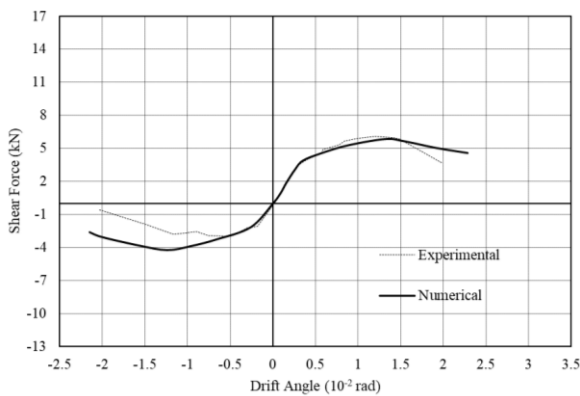
FEM analysis through ABAQUS applying quasi-static loading transverse direction of long dimension of slab, the following results are found in fig. 3 with a comparison of experimental results [7] related to shear force and deformation capacity.



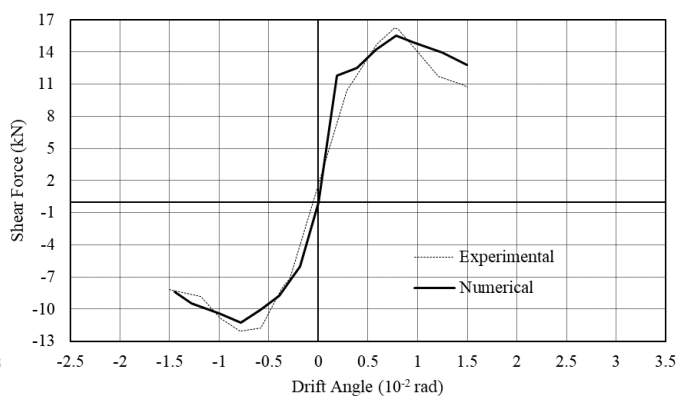
(a) Non-retrofitted (Hysteresis Curve)



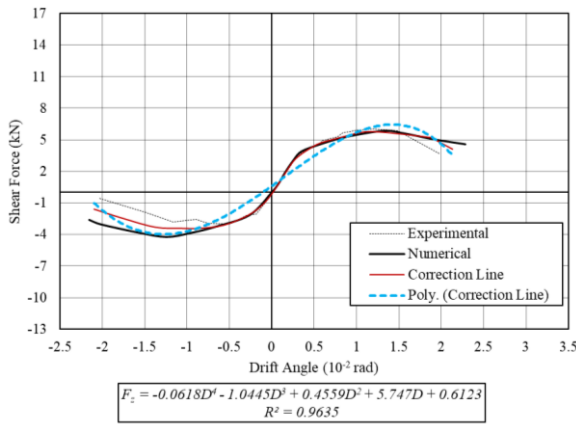
(b) Retrofitted (Hysteresis Curve)



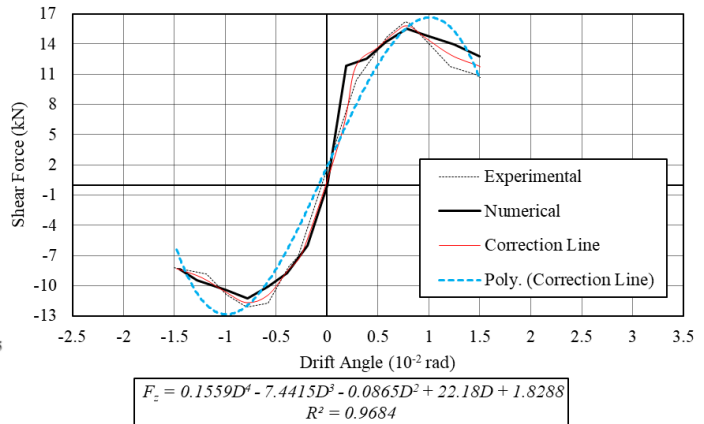
(c) Non-retrofitted (Skeleton Curve)



(d) Retrofitted (Skeleton Curve)



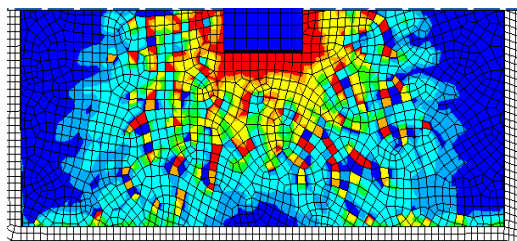
(e) Non-retrofitted (Proposed Relations)



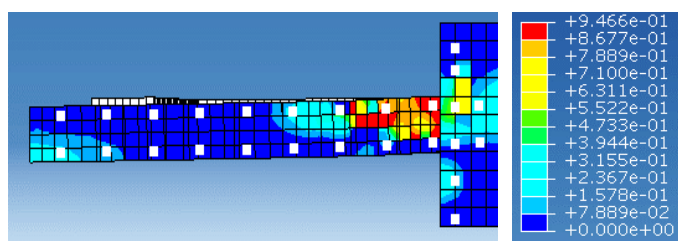
(f) Retrofitted (Proposed Relations)

Fig. 3- Comparative results of Shear Force-Drift Angle in ABAQUS simulations and experiments.

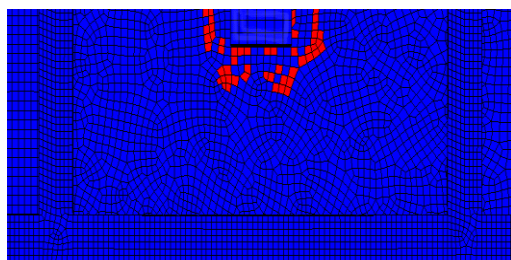
The skeleton graphs from Fig. 3(c,d) show the deviations of peaks and final stages. In case of a non-retrofitted sample, the sudden huge deformation in experiment can be an experimental error which is identified in numerical analysis. With over 95% confidence (R), two phenomenological models are developed and proposed in Fig. 3 (e,f) as shear force (F_z) respect to drift angle (D) which may describe the failure of flat plate during earthquake including analysis and design purpose. There are some differences between calculated and experimental hysteretic curves in Fig. 3(a,b), the analytical model over estimate the energy dissipating capacity of the specimen, though the stiffness degradation has been considered in the CDP material model, the calculated cycles are still plumper, which mainly accounts for the reason that the bond-slip behavior in the interfaces of both steel-concrete and reinforcement concrete is ignored in the analytical model, CDP model cannot accurately describe the crack opening and closing behavior of concrete material under cyclic loadings [4]. Importantly, the visualization of crack propagation under cyclic loading and failure pattern are identified in tension damage criteria and active yield location in fig. 4, 5 with experimental photos.



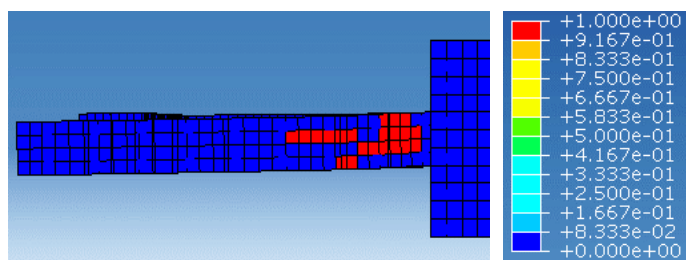
(a) Tension Damage crack propagation (Top Surface)



(b) Tension Damage crack propagation (Cut Surface)



(c) Active Yield Failure Pattern (Top Surface)



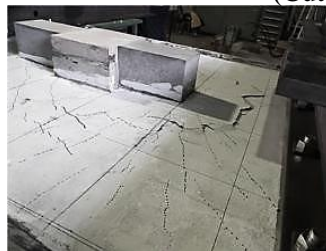
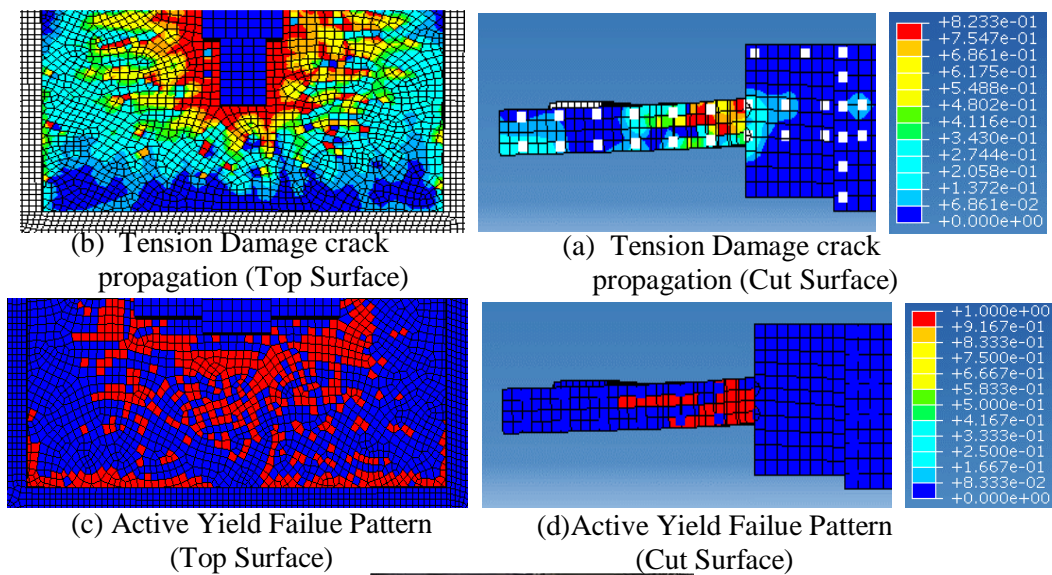
(d) Active Yield Failure Pattern (Cut Surface)



(e) Visible Failure Pattern (Experiment)[7]

Fig. 4- Crack propagations and visualization of failure pattern simulations (ABAQUS) with experimental pictorial identification of non-retrofitted specimen.

In the tension damage criteria the damage tensile strains are defined, fig. 4(a) the crack propagation lines, some top surface cracks are found at the edge due to the pressure of loading steel. The formation of tensile strain at the end shown in fig. 4(b) is basically propagating failure line due to shear stresses as the shear stress is developed maintaining 45 degree angle flat plain where tensile stress and tensile strain acting perpendicular to the shear flow surface. In case of fig. 4(c) expresses directly the punching shear failure pattern through active yield criteria, fig. 4(d) shows the inclined failure surface occurred inside the slab plain.



(e) Visible Failure Pattern (Experiment)[7]

Fig. 5- Crack propagations and visualization of failure pattern simulations (ABAQUS) with experimental pictorial identification of retrofitted specimen (wing wall).

In the tension damage criteria the damage tensile strains are defined, fig. 5(a) the crack propagation lines, some top surface cracks are found at the edge due to the pressure of loading steel. The formation of tensile strain at the end shown in fig. 5(b) is basically propagating failure line due to shear stresses as the shear stress is developed maintaining 45 degree angle flat plain where tensile stress and tensile strain acting perpendicular to the shear flow surface. It is clear from fig. 5(d) that the edge damages are only surface crack damages though



fig. 5(c) shows damage at the edge as the inside cut plain failure locations do not tend to edge locations. From the simulated failure pattern and locations are identified, counting the mesh distances the average punching failure line occurred in between effective Depth (d) and half of effective Depth distance which supports the analytical rule of punching. However, The numerical results are in agreement with the experiments conducted by Samdani *at el.* [7]

3. Results and Discussions

The shear force versus vertical drift ratio relationships from nonlinear FEM analysis applying CDP model shown in Figure 3, in which the shear force is the average value of non-retrofitted specimen. Before retrofit, the maximum load from numerical simulation was 5.98 kN compared to experimental result of 6.08 kN. The corresponding values came out to be 15.93 kN and 16.60 kN respectively after strengthening. In the maximum strength of 5.98kN of non-retrofitted specimen, the maximum drift angle is observed as 2.29×10^{-2} rad where the experiment shows 3.008×10^{-2} rad and the punching shear crack failure is identified in both simulation and experiment in figure-4. In the maximum strength of 15.93kN, the maximum drift angle is observed as 1.64×10^{-2} rad where the experiment shows 1.5035×10^{-2} rad and the punching shear crack failure is identified in both simulation and experiment in figure-5. Figure-4,5 (c, d, e) shows the punching shear failure occurred on the top surface of the slab in FEM simulation and experiment. Tension damage crack propagation shows the initiation of cracks and active yield red lines shows the punching and failure pattern. Polynomial nonlinear regression method is adopted to find the phenomenological possible relations comparing simulation and experimental results.

4. Conclusions

From this numerical simulation, the following decisions can be concluded:

- 1) The maximum strength of strengthened specimens is significantly increased compared to the non-retrofitted specimen.
- 3) Punching failure pattern due to shear stress is found in both cases and it is clear that nonlinear FEM analysis with CDP model can predict the expected scenario through visualization and output results.
- 4) A limitation of CDP in terms of energy dissipation capacity prediction is identified. Future modification of CDP model considering bond slip behaviour of RCC structure is necessary to optimize the results with the applications of ABAQUS.
- 4) More experiments are needed to avoid the statistical errors in proposing the empirical relations in such simulation for flat plate considering earthquake phenomena.

5. Acknowledgements

This research was supported by JICA/JST Science and Technology Research Partnership for Sustainable Development (SATREPS/TSUIB) project headed by Mohammad Shamim AKHTER (HBRI, Bangladesh) and Yoshiaki NAKANO (UTokyo, Japan). The authors gratefully acknowledge all supports to the research.

6. Copyrights

17WCEE-IAEE 2020 reserves the copyright for the published proceedings. Authors will have the right to use content of the published paper in part or in full for their own work. Authors who use previously published data and illustrations must acknowledge the source in the figure captions.

7. References

- [1] Karlson H & Sorensen I (2002): ABAQUS Theory Manual. Version 6.3.



- [2] Jankowiak T, Lodygowski T (2005): Identification of Parameters of Concrete Damage Plasticity Constitutive Model. Foundations of Civil and Environmental Engineering, No. 06.
- [3] Kupfer H, Hilsdorf HK, Rusch H (1979): Behavior of concrete under biaxial stresses. ACI Journal, 65, 8, 656-666.
- [4] Kui X., Qilin Z. and Bin J. (2015): Cyclic behavior of prefabricated reinforced concrete frame with infill slit shear walls. Springer Journal.
- [5] Lubliner JJ, Oliver SO, Oñate E (1989): A plastic-damage model for concrete, International Journal of Solids and Structures, 25, 3, 229-326.
- [6] Mojtaba L, Mojtaba Z, Abdol AS (2017): A new method for CDP input parameter identification of the ABAQUS software guaranteeing the uniqueness and precision. International Journal of Structural Integrity, Vol. 8 Iss 2 pp.
- [7] Samdani HMG., Takahashi S, Sanada Y, Suzuki S, Yoon R (2019): Experimental Study on a Strengthening Technique by Wing Walls for Flat Plate-Column Connections with Low-Strength Concrete. 日本建築学会近畿支部研究報告集, Vol.5, 構造系, pp.485-488.
- [8] Szczecina M. and Winnicki A. (2015): Calibration of the CDP model parameters in Abaqus. ASEM15